Electronic Supplementary Information (ESI)

For

Guanidine-Based Protic Ionic Liquids as High-Efficient Intermolecular Scissors for Dissolving Natural Cellulose

Shi-Peng Chen,[1] Jin-Long Zhu,[1] Xing-Ru Chen,[1] Zhi-Hao Wang,[1] Yong-Jie Dan,[1] Jing Wang,[1] Sheng-Yang Zhou,[2] Gan-Ji Zhong,[1] Hua-Dong Huang,[1,*] Zhong-Ming Li[1,*]

[1]*College of Polymer Science and Engineering, State Key Laboratory of Polymer Materials Engineering, Sichuan University, No. 24 South Section 1, Yihuan Road, Chengdu, 610065, China*

[2]*Nanotechnology and Functional Materials, Department of Materials Science and Engineering, The Ångström Laboratory, Uppsala University, 75103 Uppsala, Sweden;*

* Corresponding to Huang, H. (hdhuang@scu.edu.cn); Li, Z. (zmli@scu.edu.cn)

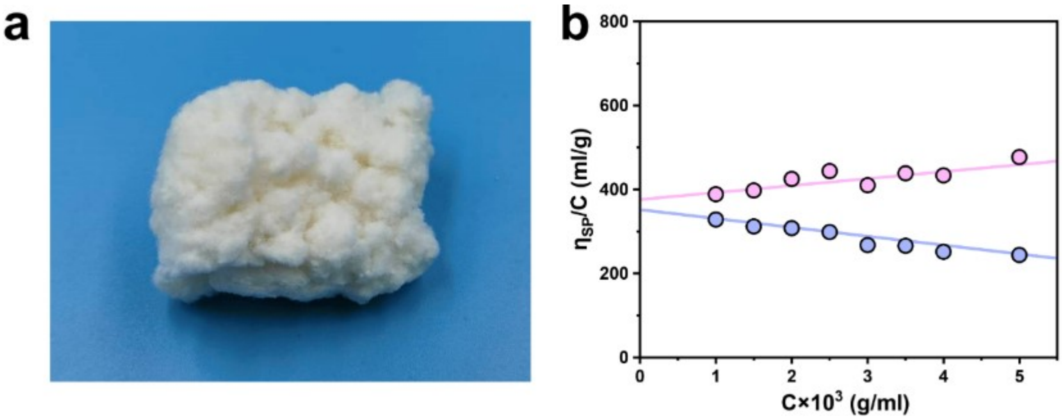

Fig. S1 **a** The digital photograph of cotton linters. **b** Relationship between [η] and concentration of cotton linters in CED (0.5M; 25 ^{o}C).

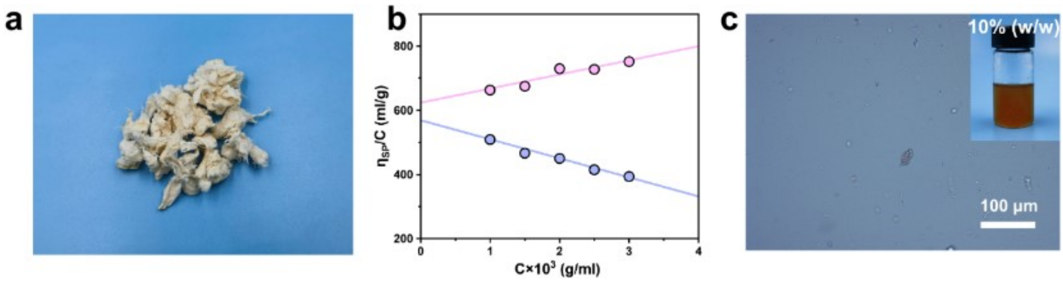

Fig. S2 **a** The digital photograph of bark pulp. **b** Relationship between [η] and concentration of bark pulp in CED (0.5M; 25 ^{o}C). **c** The POM image and digital photograph of 10% (w/w) bark pulp solution with [TMGH][MAA].

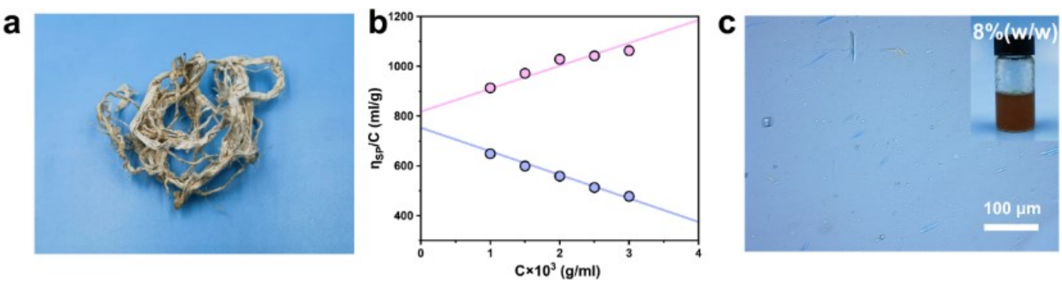

Fig. S3 **a** The digital photograph of treated bark. **b** Relationship between [η] and concentration of treated bark in CED (0.5M; 25 ^{o}C). **c** The POM image and digital photograph of 8% (w/w) treated bark solution with [TMGH][MAA].

POM is used to identify the dissolution state of cellulose in solvent through the observation of cellulose fibrils and crystals. **Fig. S4a** exhibits the undissolved state of cellulose in water. Obviously, the cellulose fibrils and crystals retain the intact morphology, suggesting that water can hardly break the strong hydrogen-bonding interaction of cellulose chains. The dissolution state of 14% (w/w) cellulose in [TMGH][MAA] solvent is shown in **Fig. S4b**, it is observed clearly via the POM that part of the cellulose fibrils remains in solvent, and the diameter of residual cellulose fibrils becomes larger than that of undissolved state, indicating a greater swelling state of residual cellulose. Therefore, 14% (w/w) cellulose is able to be dissolved partially in [TMGH][MAA] solvent, beyond its limit of dissolving capacity.

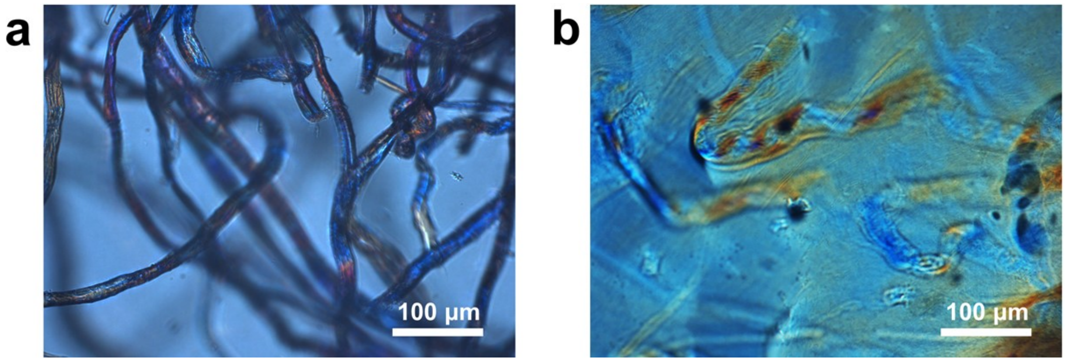

Fig. S4 The POM photographs of the cellulose dissolved in water at room temperature (**a**) and 14% (w/w) cellulose dissolved in [TMGH][MAA] solvent with the molar ratio of 6:4 at 100 ^{o}C (**b**).

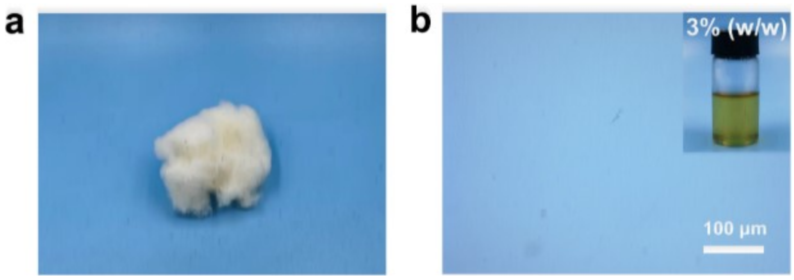

Fig. S5 **a** The digital photograph of cotton fibers. **b** The POM image and digital photograph of 3% (w/w) cotton fibers solution with [TMGH][MAA].

Table S1 The cellulose solubility of different solvents.

Raw material	Solvent[a]	Temperature (°C)	Solubility[b] (wt%)	Ref.
Disintegrated Cotton Linters (DP=600)	NMMO	140	25.9	1
Cotton Linters (DP=1130)	LiCl/DMAc	150	13.0	2
Cotton Linter Pulp (M_η=11.4x10^4)	NaOH/Urea/H_2O	-12	4.0-5.0	3
Cotton Linter Pulps (DP=667)	$BzEt_3NOH/H_2O$	-24	10.5	4
MCC (DP=145)	ChOH/Urea	70	9.51	5
Dissolved Pulp (DP=650)	AmimCl	80	14.5	6
Dissolving Pulp (DP=1000)	BmimCl	100	10.0	7
MCC (DP=156)	[DBUH][$CH_3CH_2OCH_2COO$]	80	18.1	8

MCC (DP=292)	DBN-PyO-4	70	14.1	9
Cotton Linters (DP=741)	[TMGH][MAA]	80	11.5	This work
Bark pulp (DP=1295)	[TMGH][MAA]	80	9.1	This work
Treated bark (DP=1743)	[TMGH][MAA]	80	7.4	This work
Cotton fibers (DP=10,000-15,000)	[TMGH][MAA]	80	2.9	This work

[a] The solvents of $BzEt_3NOH/H_2O$, ChOH/Urea, $[DBUH][CH_3CH_2OCH_2COO]$ and DBN-PyO-4 represent Benzyltriethyl ammonium aqueous solution, choline hydroxide/urea deep eutectic solvent, 1,5-diazabicyclo[4.3.0]non-5-enium ethoxyacetate and 1,5-diazabicyclo[4.3.0]non-5-enium pyridine N-oxide, respectively.

[b] The cellulose solubility of solvents is expressed by the ratio of dissolved cellulose mass to the total mass of dissolved cellulose and solvents.

Table S2 The ^{13}C-NMR Chemical Shifts of Pure [TMGH][MAA] Solvent and Cellulose Solution (5:5, TMG/MAA molar ratio) at Room Temperature.

Sample	δ(ppm)				
	I-C	II-C	III-C	IV-C	V-C
[TMGH][MAA]	39.72	162.14	57.87	72.91	172.76
Cellulose-[TMGH][MAA]	39.73	161.86	57.94	72.66	173.10
Δδ	+0.01	-0.28	+0.07	-0.25	+0.34

Table S3 The ^{13}C-NMR Chemical Shifts of Pure [TMGH][MAA] Solvent and Cellobiose Solution (5:5, TMG/MAA molar ratio) at Room Temperature.

Sample	δ(ppm)				
	I-C	II-C	III-C	IV-C	V-C
[TMGH][MAA]	39.73	162.14	57.87	72.92	172.73
Cellobiose-[TMGH][MAA]	39.74	161.92	57.95	72.71	173.44
Δδ	+0.01	-0.22	+0.08	-0.21	+0.71

Table S4 The ^{13}C-NMR Chemical Shifts of Pure Cellobiose and Cellobiose Solution (5:5, TMG/MAA molar ratio) at Room Temperature.

Sample	δ(ppm)																		
	C1	**C1′α**	**C1′β**	**C2**	**C2′α**	**C2′β**	**C3**	**C3′α**	**C3′β**	**C4**	**C4′α**	**C4′β**	**C5**	**C5′α**	**C5′β**	**C6α**	**C6β**	**C6′α**	**C6′β**
Cellobiose	103.61	92.47	97.09	75.49	72.51	71.86	76.91	74.94	73.75	70.27	81.43	81.17	77.21	70.48	75.17	61.47	61.45	60.99	60.93
Cellobiose-[TMGH][MAA]	103.83	92.63	97.83	75.32	71.99	71.91	76.86	73.96	72.93	70.18	81.35	81.35	77.65	70.31	74.62	61.22	61.19	61.12	61.10
Δδ	+0.22	+0.16	+0.74	-0.17	-0.52	+0.05	-0.05	-0.98	-0.82	-0.09	-0.08	+0.18	+0.44	-0.17	-0.55	-0.25	-0.26	+0.13	+0.17

The ^{1}H-NMR spectroscopy of [TMGH][MAA] solvent and cellulose solution in [TMGH][MAA] at the TMG/MAA molar ratio of 5:5 is shown in **Fig. S6**. As the cellulose is dissolved in [TMGH][MAA] solvent, the proton signal of =NH becomes broader, which deduces that [TMGH][MAA] solvent has strong interaction with cellulose via hydrogen bonds. Moreover, this signal shifts downfield from 8.39 ppm to 8.45 ppm. It indicates that the proton in =NH of [TMGH] forms hydrogen bonds with the oxygen atoms in -OH of cellulose, causing the decrease of electron cloud density.

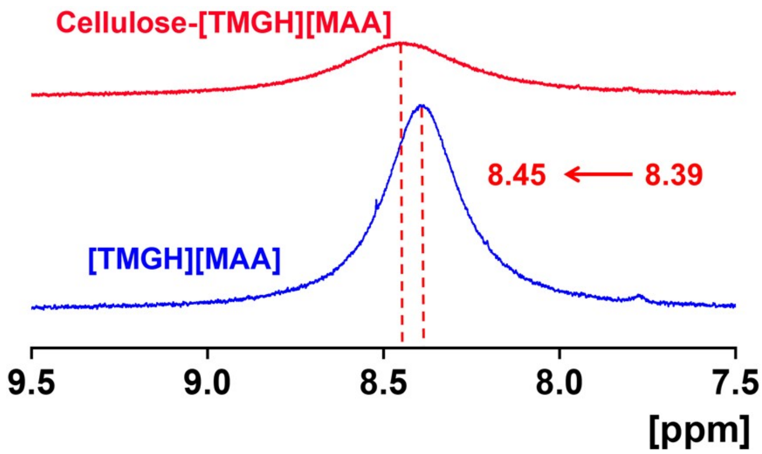

Fig. S6 ^{1}H-NMR spectrum of the cellulose solution in [TMGH][MAA] solvent and the corresponding pure [TMGH][MAA] solvent with TMG/MAA molar ratio of 5:5.

The ^{1}H-NMR spectroscopy of cellobiose and cellobiose/[TMGH][MAA] solution with 5:5 TMG/MAA molar ratio is shown in **Fig. S7**. The signals in the range of 2.9 ppm–4.0 ppm belong to the backbone hydrogen atoms of cellobiose. With cellobiose dissolved in [TMGH][MAA] solvent, the peaks of 2β-H, 2'β-H, 3β-H, 3'β-H, 6β-H and 6'β-H shift upfield, indicating that the formation of hydrogen bonds between [TMGH][MAA] solvent and -OH of C2, C2', C3, C3', C6 and C6' in cellobiose increases the electron cloud density of the corresponding cellobiose backbone hydrogen atoms.

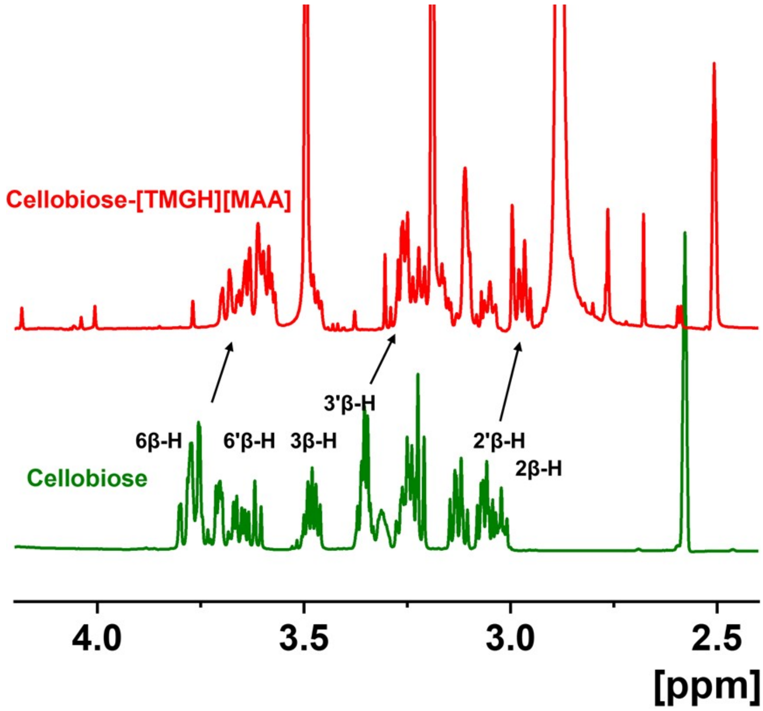

Fig. S7 [1]H-NMR spectrum of pure cellobiose and the cellobiose solution in [TMGH][MAA] solvent with 5:5 TMG/MAA molar ratio.

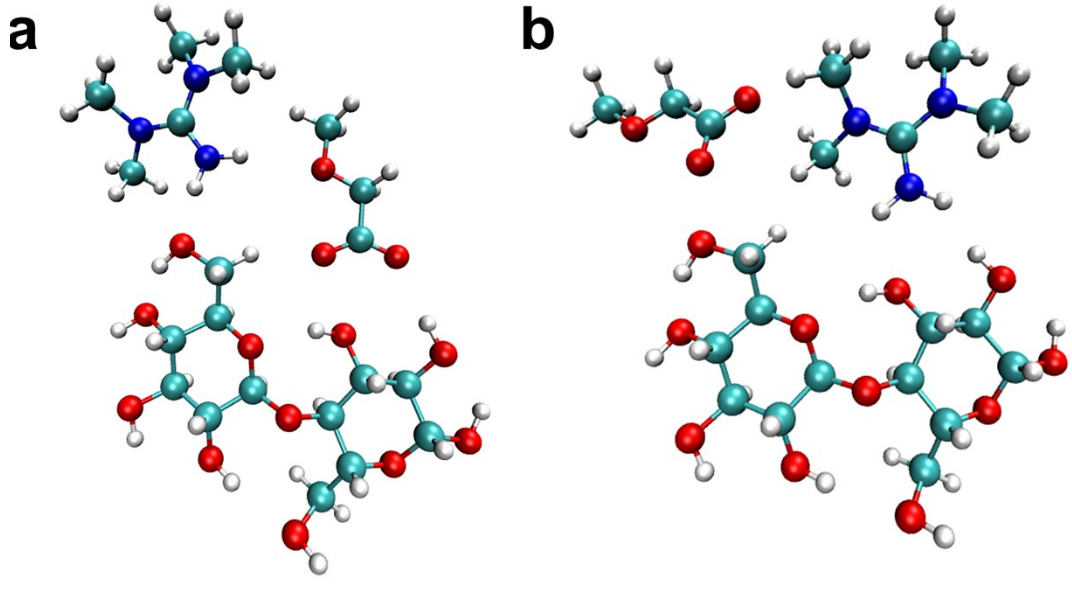

Fig. S8 Initial structure A (**a**) and structure B (**b**) of [TMGH][MAA] and cellobiose for DFT calculation.

Table S5 Electron Density (ρ_{BCP}) and its Laplacian ($\nabla^2\rho_{BCP}$) at the BCPs of Bonds, Obtained by AIM Theory.

Structure	Sort	Bond	ρ(bcp)	∇^2ρ(bcp)
A	[MAA]-Cellobiose	O-H···O	0.03829	0.1155
	[MAA]- Cellobiose	C···O	0.00917	0.03727
	[MAA]- Cellobiose	C-H···O	0.00184	0.006069
	[TMGH]- Cellobiose	N-H···O	0.02510	0.09788
	[TMGH]-[MAA]	N-H···O	0.03342	0.1166
	[TMGH]-[MAA]	C-H···O	0.009072	0.03857
	[TMGH]-[MAA]	C-H···O	0.006193	0.02189
	[TMGH]-[MAA]	C-H···O	0.007324	0.02604
B	[TMGH]- Cellobiose	N-H···O	0.005183	0.02204
	[TMGH]- Cellobiose	N-H···O	0.03177	0.1133
	[TMGH]- Cellobiose	C-H···O	0.005516	0.02183
	[TMGH]-[MAA]	C-H···O	0.01027	0.03770
	[TMGH]-[MAA]	C-H···O	0.005873	0.01955
	[TMGH]-[MAA]	C-H···O	0.01138	0.04159

The conductivity of the mixture of [TMGH][MAA] solvent and 1 wt% water is shown in **Fig. S9a**, and the shape of curve surface is consistent with that of pure solvent in **Fig. S3a**. The conductivity increases with the increase of temperature. In addition, as the TMG/MAA molar ratio increases, the conductivity first increases and then decreases beyond the TMG/MAA molar ratio of 7:3. **Fig. S9b** presents the viscosity of the mixture of [TMGH][MAA] solvent and 1 wt% water from 30 °C to 100 °C. As expected, the viscosity decreases with the increased temperature.

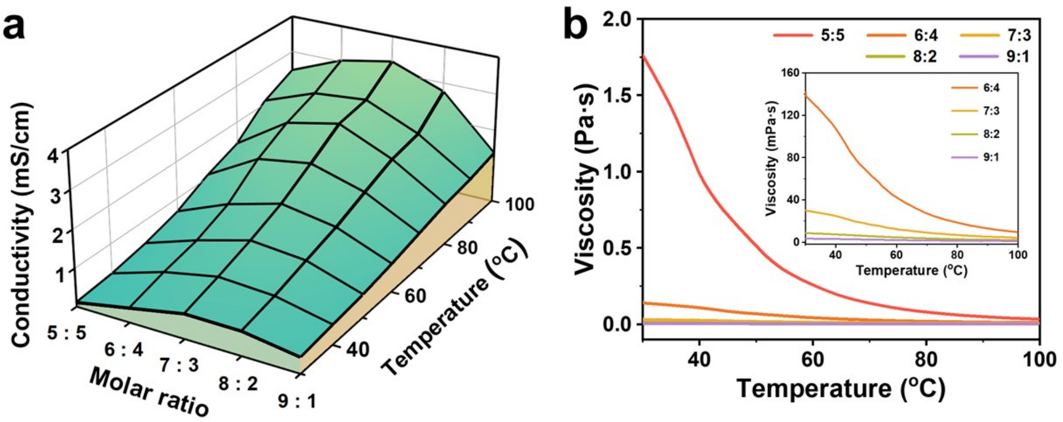

Fig. S9 a The effect of temperature on electrical conductivity of the mixture of the [TMGH][MAA] solvent and 1 wt% water. **b** Viscosity of the mixture of [TMGH][MAA] solvent with various TMG/MAA molar ratios and 1 wt% water as a function of temperature from 30 °C to 100 °C. The inset shows the partial enlarged viscosity curves of the mixture with the TMG/MAA molar ratios from 6:4 to 9:1.

The viscosity-shearing rate curves of [TMGH][MAA] solvent and 5% (w/w) cellulose solution with various TMG/MAA molar ratios are shown in **Fig. S10**. As shown in **Fig. S10a**, the viscosity of [TMGH][MAA] solvent remains constant with the increase of shearing rate, exhibiting a characteristic of Newtonian fluids. When the TMG/MAA molar ratio increases to 7:3, the viscosity of [TMGH][MAA] solvent is obtained to be a particularly lower value of 67.3 mPa·s compared to imidazolium-based ILs (AmimCl: 685 mPa·s at 30 °C;[6] BmimCl: 11000 mPa·s at 30 °C[10]), which shows better fluidity and is more favor of cellulose dissolution. In **Fig. S10b**, the viscosity of cellulose solution decreases with increased shearing rate, exhibiting a feature of non-Newtonian fluids. It suggests that cellulose is dissolved effectively into [TMGH][MAA] solvent. With the same tendency as that of solvent, the viscosity of cellulose solution decreases with the increase of TMG/MAA molar ratio. Due to the weak cellulose dissolution capacity of [TMGH][MAA] solvent with 9:1 molar ratio, the viscosity of corresponding 5% (w/w) cellulose solution could not be measured. In addition, at a low shear rate, the viscosity of 5% (w/w) cellulose solution with the TMG/MAA molar ratio of 7:3 is in the range of medium viscosity fluids (5～50 Pa·s), which exhibits a good processability.

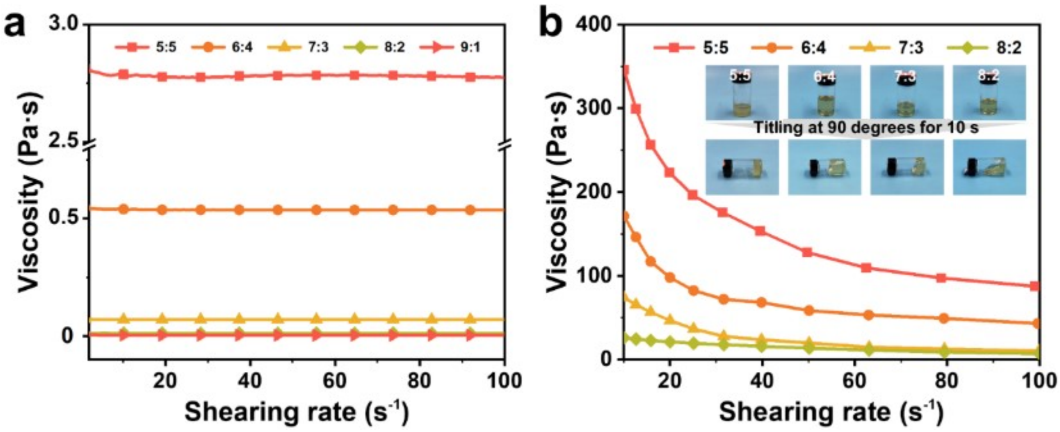

Fig. S10 **a** Viscosity as a function of shearing rate for [TMGH][MAA] solvent. **b** Viscosity as a function of shearing rate for 5% (w/w) cellulose solution with various TMG/MAA molar ratios at room temperature, and the inset is the flowing state of cellulose solution with various TMG/MAA molar ratios after tilting at 90^{o} for 10 s.

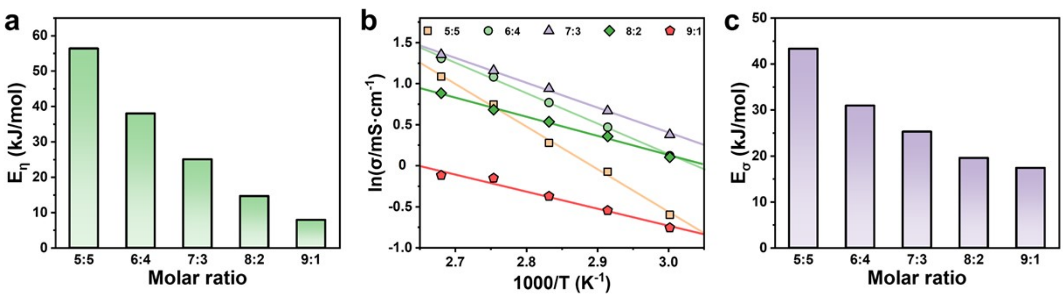

Fig. S11 a Dependencies of flow activation energy (E_η) on TMG/MAA molar ratio in [TMGH][MAA] solvent. **b** Arrhenius fitted lines of lnσ versus 1/T for [TMGH][MAA] solvent. **c** Dependencies of activation energy for electrical conduction (E_σ) on TMG/MAA molar ratio in [TMGH][MAA] solvent.

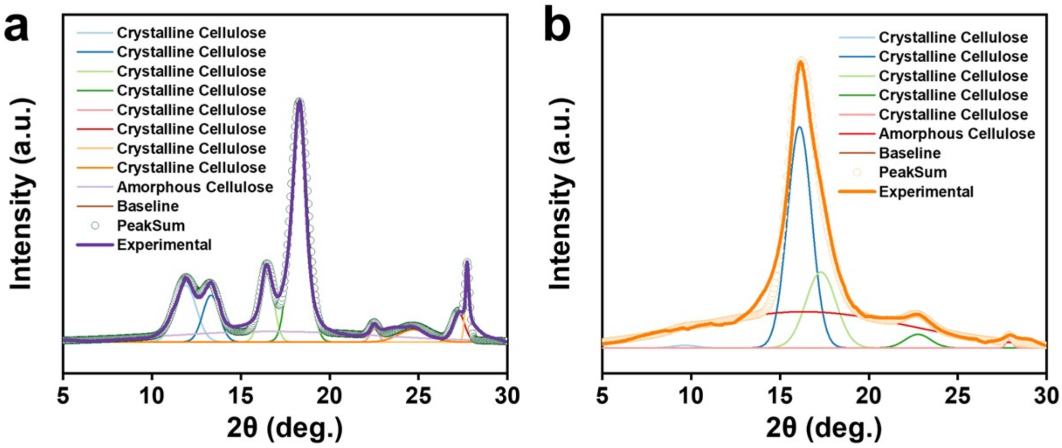

Fig. S12 Deconvolution of WAXD patterns for original cellulose (**a**) and regenerated cellulose film (**b**).

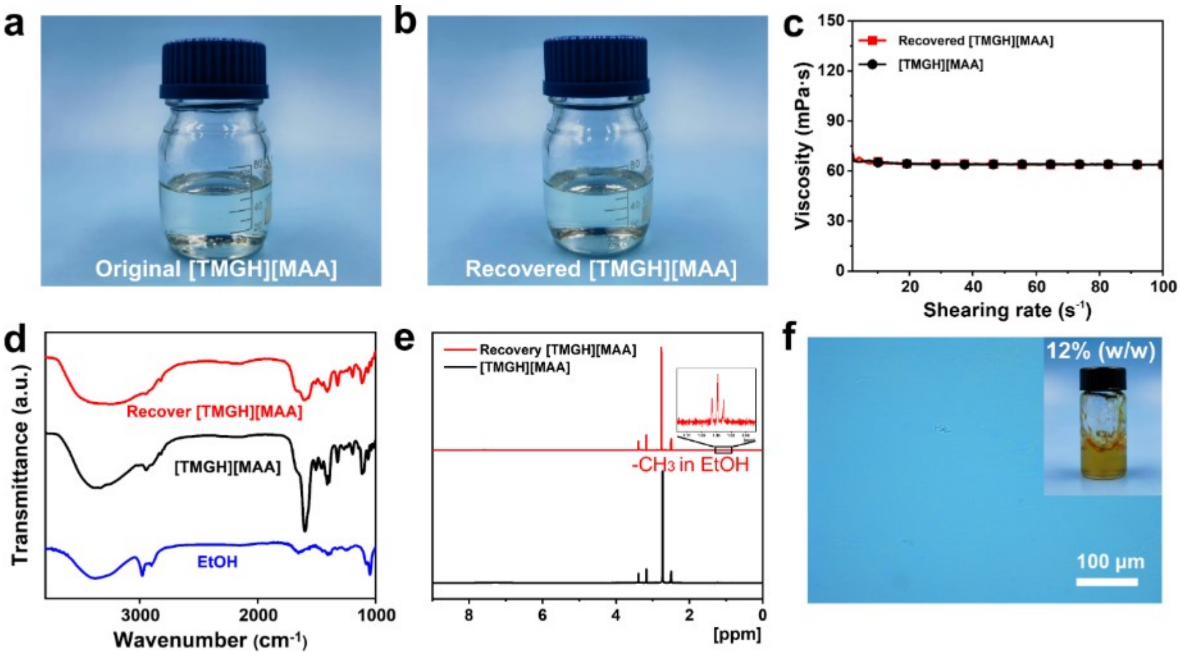

Fig. S13 The digital photograph of original [TMGH][MAA] (**a**) and recovered

[TMGH][MAA] (**b**). **c** Viscosity as a function of shearing rate for original [TMGH][MAA] and recovered [TMGH][MAA]. **d** ATR-FTIR spectra of original [TMGH][MAA], recovered [TMGH][MAA] and EtOH. **e** ^{1}H-NMR spectrum of original [TMGH][MAA] and recovered [TMGH][MAA]. **f** The POM image and digital photograph of 12% (w/w) cotton linters solution with recovered [TMGH][MAA].

Supplementary References

1. H. Chanzy and A. Peguy, *J. Polym. Sci. Polym. Phys. Ed.*, 1980, **18**, 1137-1144.
2. C. L. McCormick, P. A. Callais and B. H. Jr. Hutchinson, *Macromolecules*, 1985, **18**, 2394-2401.
3. J. Cai and L. Zhang, *Macromol. Biosci.*, 2005, **5**, 539-548.
4. Y. Wang, L. Liu, P. Chen, L. Zhang and A. Lu, *Phys. Chem. Chem. Phys.*, 2018, **20**, 14223-14233.
5. Y. Zhong, J. Wu, H. Kang and R. Liu, *Green Chem.*, 2022, **24**, 2464-2475.
6. H. Zhang, J. Wu, J. Zhang and J. He, *Macromolecules*, 2005, **38**, 8272-8277.
7. R. P. Swatloski, S. K. Spear, J. D. Holbrey and R. D. Rogers, *J. Am. Chem. Soc.*, 2002, **124**, 4974-4975.
8. X. Li, H. Li, Z. Ling, D. Xu, T. You, Y.-Y. Wu and F. Xu, *Macromolecules*, 2020, **53**, 3284-3295.
9. Q. Liu, H. Yu, T. Mu, Z. Xue and F. Xu, *Carbohydr. Polym.*, 2021, **272**, 118454.
10. K. R. Seddon, A. Stark and M.-J. Torres, in *Clean Solvents*, American Chemical Society, 2002, vol. 819, ch. 4, pp. 34-49.